


 Cite this: *RSC Adv.*, 2020, 10, 9356

## Bio-nanoparticle assembly: a potent on-site biolarvicidal agent against mosquito vectors

 Nazima Sultana,<sup>a</sup> Prasanta K. Raul,<sup>ID</sup> \*<sup>a</sup> Diganta Goswami,<sup>a</sup> Dipankar Das,<sup>b</sup> Saidul Islam,<sup>c</sup> Varun Tyagi,<sup>a</sup> Bodhaditya Das,<sup>a</sup> Hemanta K. Gogoi,<sup>a</sup> Pronobesh Chattopadhyay<sup>a</sup> and Pakalapati S. Raju<sup>a</sup>

**Background:** Vector-borne diseases such as malaria, dengue, yellow fever, encephalitis and filariasis are considered serious human health concerns in the field of medical entomology. Controlling the population of mosquito vectors is one of the best strategies for combating such vector-borne diseases. However, the use of synthetic insecticides for longer periods of time increases mosquito resistance to the insecticides. Recently, the search for new environmentally friendly and efficient insecticides has attracted major attention globally. With the evolution of material sciences, researchers have reported the effective control of such diseases using various sustainable resources. The present investigation demonstrates a potent on-site biolarvicidal agent against different mosquito vectors such as *Aedes albopictus*, *Anopheles stephensi* and *Culex quinquefasciatus*. **Methods:** Stable and photo-induced colloidal silver nanoparticles were generated *via* the surface functionalization of the root extract of *Cyprus rotundas*. Characterizations of the nanoparticles were performed using assorted techniques, such as UV-visible spectroscopy, FTIR spectroscopy, DLS and HRTEM. The bioefficacy of the synthesized nanoparticles was investigated against different species of mosquito larvae through the evaluation of their life history trait studies, fecundity and hatchability rate of the treated larvae. Histopathological and polymerase chain reaction-random amplified polymorphic DNA (RAPD) analyses of the treated larvae were also examined to establish the cellular damage. **Results:** The synthesized nanoparticles showed remarkable larvicidal activity against mosquito larvae in a very low concentration range (0.001–1.00) mg L<sup>-1</sup>. The histopathological study confirmed that the present nanoparticles could easily enter the cuticle membrane of mosquito larvae and subsequently obliterate their complete intestinal system. Furthermore, RAPD analysis of the treated larvae could assess the damage of the DNA banding pattern. **Conclusion:** The present work demonstrates a potent biolarvicidal agent using sustainable bioresources of the aqueous *Cyprus rotundas* root extract. The results showed that the synthesized nanoparticles were stable under different physiological conditions such as temperature and photo-induced oxidation. The effectiveness of these materials against mosquito larvae was quantified at very low dose concentrations. The present biolarvicidal agent can be considered as an environmentally benign material to control the mosquito vectors with an immense potential for on-site field applications.

 Received 28th November 2019  
 Accepted 11th February 2020

DOI: 10.1039/c9ra09972g

[rsc.li/rsc-advances](http://rsc.li/rsc-advances)

### 1. Introduction

Vector-borne diseases, for example, malaria, dengue, yellow fever and filariasis are considered to be serious health issues. Mosquito species belonging to the genera *Aedes albopictus*,

*Anopheles stephensi* and *Culex quinquefasciatus* play significant roles in the transmission of such vector-borne diseases. *Anopheles stephensi* is the primary malaria vector found in India and other Asian countries and transmits filariasis.<sup>1</sup> The *Aedes aegypti* vector transmits several yellow fevers like dengue, chikungunya, viruses and other diseases.<sup>2</sup> *Culex quinquefasciatus* is an important vector of lymphatic filariasis.<sup>3</sup> These species are found abundantly in many tropical areas of the world and breed very fast in drains and stagnant water reservoirs; their development involves the holometabolous life cycle, which includes four life stages: eggs, larvae, pupae and adults. Although the use of synthetic insecticides can interrupt these disease transmissions, the repeated use of insecticides can easily destroy the ecosystem and lead to a resurgence of the mosquito

<sup>a</sup>Defence Research Laboratory, DRDO, Post bag no. 2, Tezpur-784001, Assam, India. E-mail: prasanta.drdo@gmail.com; sultana.nazima47@gmail.com; digs78@gmail.com; bodhadityaj@gmail.com; varunbhardwaj.tyagi@gmail.com; gogoi\_hk@yahoo.com; chattopadhyay.drdo@gmail.com; psrajusci@yahoo.com; Fax: +91-3712-258534; Tel: +91-3712-258836

<sup>b</sup>Sri Sankardeva Nethralaya, Beltola, Guwahati-781028, Assam, India. E-mail: dr\_dasdipankar@yahoo.com

<sup>c</sup>College of Veterinary Science, Assam Agricultural University, Khanapara, Guwahati – 781022, India. E-mail: isaidul@yahoo.com



population.<sup>4,5</sup> In addition, a number of challenging medical treatments have been reported to cure an infected person.<sup>6</sup> However, the development of control programs for mosquito vectors at their earlier stage is more suitable to prevent such transmitted vector-borne diseases.<sup>7</sup> Also, the targeting of the larvae is considered an effective strategy due to their lower mobility in breeding habitats. Since the past few decades, researchers have been searching for eco-friendly, biodegradable and economically viable alternatives to chemical insecticides to suppress the population of various mosquito disease vectors.<sup>8,9</sup>

With the evolution of material sciences, nanoparticles are now considered as a promising candidate to control vector-borne diseases.<sup>10</sup> It is considered to be the latest promising platform to help reach that goal with a wide range of benefits, including increased bioefficacy, durability and controlled delivery to the specific targets. The use of efficient nanoparticles with improved physicochemical properties can help to reduce the serious environmental issues of larvicidal agent.<sup>10–16</sup> Studies with silver nanoparticles have been done extensively against several different types of mosquito vectors.<sup>10,17,18</sup> Various chemical and physical methods are used for the synthesis of nanoparticles. The use of plant sources-based bioactive organic chemicals has gained more attention to synthesize silver nanoparticles.<sup>19–23</sup> Phytochemical approaches for the synthesis of silver nanoparticles are considered to be a promising method for controlling mosquito vector-borne diseases due to their low toxicity and cost effectiveness.<sup>24</sup> Various intersections have been highlighted between biotechnology and nanotechnology *via* the development of environmental benign technologies in the field of material sciences, whereby such materials can serve as defence chemicals, like insecticides, anti-feedants, repellents, oviposition deterrents, growth inhibitors, and moulting hormones as well as attractants due to the occurrence of secondary metabolites.<sup>25</sup> Despite the spectacular activities of silver nanoparticles, their large-scale utility is not yet considered due to the requirement of high dose concentrations, which can further induce toxicological effects on non-targeted organisms present in the environment.<sup>26</sup> Therefore, the utilization of highly biocompatible and biodegradable polymeric materials to synthesize the nanoparticles may be a far-reaching goal to overcome such environmental risk factors.

The *Cyprus rotundas* plant is an important bioresource for nutrition and medicine. It is a carbohydrate-rich leguminous root species and such polysaccharide-based nutgrass plants are widely available in South Asia. It is indigenous to India, available mostly in tropical, subtropical and temperate regions. The extreme black tubers of the *Cyprus rotundas* plant with a characteristic odour have staple carbohydrate-based contents, like acyperone, b-selinene, cyperene, patchoulenone, sugeonol, kobusone and isokobusone, which are significant for medicinal use, especially as a larvicidal.<sup>27</sup> Therefore, in this context we aimed to prepare a stable silver nano-biocomposite material using a facile method with *Cyprus rotundas* root extract. We observed an excellent effectiveness of the synthesized biol-arvicidal agent against various mosquito disease vectors and the obtained results are presented here.

## 2. Experimental section

### 2.1 Materials and methods

*Cyprus rotundas* root were collected from the Defence Research Laboratory garden in Tezpur, Assam, India. They were washed with tap water several times to remove dust particles and were then sun dried. The dried *Cyprus rotundas* roots were further ground to make fine powder using a domestic blender.

### 2.2 Biosynthesis of silver nanoparticles

*Cyprus rotundas* root powder (2 g) was heated with 100 mL of water at 50 °C for 1 h and then filtered using muslin cloth. Next, 100 mL of 0.01 (M) AgNO<sub>3</sub> solution was added drop-wise with 50 mL root extract in a conical flask and with continuous stirring at 50 °C for up to 2 h. After the termination of the reaction time, the mixture was allowed to cool down at room temperature and finally a dark brown colloidal solution was obtained. The collected solution was filtered using a muslin cloth and centrifuged at 960 × *g* for 10 min to remove any undesired large particles. The product was vacuum dried at room temperature. The dried product was further dissolved in water to make 1000 mg L<sup>-1</sup> stock solution.

### 2.3 General experimental procedures

A UV-visible spectrophotometer (U2001, Hitachi, Japan) was used for the detection of the surface plasmon resonance (SPR) peaks. The formation of silver nanoparticles was preliminarily confirmed with the help of dynamic light scattering (DLS) measurements using a Malvern Nano ZS instrument at 633 nm (a 4 mW He Ne laser was used) and 90° scattering angle. The prepared colloidal solution was filtered through a 0.22 μm membrane filter prior to the measurements. The scattering intensity data were processed using instrumental software to obtain the average hydrodynamic diameter (*d<sub>H</sub>*) of the particles in the solution. The chemical functionalities of the nano-materials solutions were identified using Fourier transform infrared spectrometry (FTIR) (Bruker, Model Alpha Eco-ATR) with the accumulation of 15 scans. The spectra were recorded within the range of 500–4000 cm<sup>-1</sup>. The resolution of the spectra was set within the range of 8–2.0 cm<sup>-1</sup>. Initially, a small amount of the lyophilized sample was mixed with 1% KBr powder and ground to reduce the particle size. High-resolution transmission electron microscopy (HRTEM) images of the solution were taken on a JEOL microscope at an operating voltage of 200 kV. The sample was prepared for HRTEM by dropping aqueous suspensions of the nanoparticles onto Cu grids coated with a holey carbon film followed by solvent evaporation.

### 2.4 Mosquito larvae

Larval strains of *Aedes albopictus*, *Aedes aegypti*, *Culex quinquefasciatus* and *Anopheles stephensi* were collected from the mosquito culture facility of the Defence Research Laboratory, Tezpur, India. The mosquito larvae were maintained at 28 ± 2 °C and 75–85% relative humidity under 14 : 10 (light : dark).



They were fed with a mixture of 1 : 3 (dog biscuits : yeast extract) for their survival.

### 2.5 Larvicidal activity of the silver nanoparticles

The synthesized silver nanoparticles were subjected to a dose-response bioassay for larvicidal activity against *Aedes albopictus*, *Aedes aegypti*, *Culex quinquefasciatus* and *Anopheles stephensi* species of the larvae. For the bioassay test, initially 20 numbers of 3<sup>rd</sup> and 4<sup>th</sup> instars larvae were taken in a 100 mL beaker. Different concentrations of silver nanoparticles ranging from 0.01–5.0 mg L<sup>-1</sup> were prepared to study the larvicidal activity against the mosquito larvae. The control was set up with deionized water and kept for 24 h observation. The numbers of dead larvae were counted after 24 h of exposure and the percentage mortality was reported from the average of three replicates. Mortality was calculated using Abbott's formula.<sup>28</sup> The dose-response data were subjected to probit regression analysis using IBM SPSS Statistics software.<sup>29</sup> Lethal dose concentrations at the upper confidence limit (LC<sub>90</sub>) and at the lower confidence limit (LC<sub>50</sub>) were calculated with 95% confidence intervals.

### 2.6 Life history traits studies of the mosquito vectors

*Aedes albopictus* and *Culex quinquefasciatus* larvae were treated with silver nanoparticles and their complete life history traits were studied. Adult mosquitoes were maintained in optimum conditions at 28 ± 2 °C and 75–85% relative humidity under 14 : 10 (light : dark) photoperiod.<sup>30</sup> Male and female mosquitoes were housed together in the same size of cage (30 × 30 × 30 cm) for about one week in order to mate. Honey-soaked cotton pads were provided as a sugar source to them prior to a blood meal. Mated females were collected and fed upon rabbit blood in order to undergo egg maturation prior to testing.

### 2.7 Histological studies of the nanoparticle-treated larvae

For histological tests, both the silver nanoparticles-treated and untreated third instars larvae of *Aedes albopictus* were taken from the laboratory colony. The LC<sub>50</sub> dose concentrations of the treated larvae were incorporated after 24 h exposure and kept for examination. Afterwards, they were fixed with 10% formaldehyde solution for up to 24 h and then dehydrated using an increasing acetone gradient, *i.e.* 30–100%. The treated larvae were embedded and cut with glass knives in a rotary microtome. The sections were stained with haematoxylin-eosin, analyzed and photographed using a photomicroscope.

### 2.8 DNA extraction of the silver nanoparticles-treated larvae

DNA from the mosquito larvae was extracted using the reported method by Ballinger-Crabtree *et al.*<sup>31,32</sup> Each adult female mosquito was ground with 200 µL lysis buffer (100 mM Tris-HCl, pH 8.0; 1% sodium dodecylsulphate; 50 mM NaCl; 50 mM EDTA). The mixture was kept immediately on ice for 15 min followed by heating at 65 °C for 30 min. Subsequently, the homogenous mixture was further treated with 30 µL of 5 M potassium acetate for 1 h at 10 °C followed by centrifugation at

~13 000 rpm. The suspension was extracted by chilled ethanol and kept overnight at -20 °C. The suspension was further centrifuged at 13 000 rpm at 10 °C and the precipitated DNA was washed twice with 70% ethanol at room temperature. The pelleted DNA were kept for air drying and finally dissolved in 50 µL TE buffer. Concentrations of DNA extracted from various larvae were determined using spectrophotometer.

### 2.9 Polymerase chain reaction (PCR) and random amplified polymorphic DNA (RAPD)

We screened 20 different numbers of 10 mole oligonucleotide RAPD primers. Out of these, only two primers were assigned here as primer 1 (GTGGCTTGGA) and primer 2 (GTAAACCGCC), which showed good results. These were selected for the reared *Aedes albopictus* mosquito strains in our laboratory. RAPD amplification was performed with a 10 µL PCR mixture containing 10 mM PCR buffer at pH 9.0, 50 mM MgCl<sub>2</sub>, 2 mM dNTP, 0.2 (M) primer and 0.5 U of Tag DNA polymerase. Sterile deionized water was used for the volume make-up. 10 mg of extracted DNA was also added in to each PCR tube. The reaction mixture was given a short spin for thoroughly mixing the cocktail of components. The PCR tubes were loaded onto a thermal cycler (iCycler, Bio-Rad PCR System) for 4 min at 94 °C, followed by 35 cycles of 1 min at 94 °C, 1 min at 40 °C and 2 min at 72 °C. The final extension step was performed at 72 °C for 10 min.

### 2.10 Agarose gel electrophoresis

The amplification products were analyzed by the electrophoresis method using 1% agarose gel (w/v).<sup>33</sup> Along with the PCR-amplified products, 100 bp DNA ladders were used as the standard marker and subjected to electrophoresis using 1% agarose gel in 0.5 × TAE buffer and then stained using ethidium bromide solution. The molecular sizes of the markers were 1000, 900, 800, 700, 600, 500, 400, 300, 200 and 100 bp. The amplified pattern was visualized on a UV trans-illuminator and then photographed. Polymorphism was evidenced both in the presence or absence of DNA fragments between the samples. The RAPD profiles of the treated larvae were evaluated using the same 1% agarose gel run for h at 100 volts followed by 80 volts for about 3 h with 0.5 × TAE buffer.

## 3. Results and discussion

### 3.1 Origin of the silver nanoparticles

*Cyperus rotundas* root extract was used as a precursor to synthesize silver nanoparticles in the present work. In general, plant-based materials contain an untapped reservoir of carbohydrate sources, like cellulose, pectin, chitin, starch, chitosan and many more that can be used as templates for the synthesis of nanoparticles. Therefore, during the hydrolysis process, an aqueous extract of the material decomposes carbohydrate molecules and forms surface-functionalized circumstances by generating different functional groups, such as hydroxyl, carbonyl, carboxyl and epoxy groups, in the solution mixture.<sup>10</sup> This process helps to liberate a substantial amount of protons



and electrons to reduce the metal ions.<sup>34</sup> *Cyprus rotundas* contains more than 35% carbohydrate content.<sup>35,36</sup> During the hydrolysis in the extract preparation, the released protons and electrons help in the nucleation process of  $\text{Ag}^+$  to  $\text{Ag}^0$  and generate a water soluble stable colloidal nanoparticles solution. Initially, we prepared a saturated solution of *Cyprus rotundas* root extract using approximately 2 g of dried *Cyprus rotundas* root powder. Then, we used varying amounts of root extract, *i.e.* 10 mL, 35 mL, and 50 mL, and added this drop-wise in 0.01 M of  $\text{AgNO}_3$  solution. The mixtures were further kept for 2 h by monitoring the colour changes and then, after the completion of 2 h, we measured the sizes (hydrodynamic diameter) of the nanoparticles from DLS measurements, and their respective results are shown Fig. 1. It was seen here that the obtained particle size was higher, *i.e.* in the  $103 \pm 0.01$ – $214 \pm 0.04$  nm range, by reducing the amount of root extract. The polydispersity index of the solution was found to be  $0.662 \pm 0.02$ . Therefore, in the present study, we optimized the minimum amount of root extract, *i.e.* at 50 mL, and used it for the synthesis of stable silver nanoparticles within a very short period of time.

### 3.2 Characterization of the silver nanoparticles

The formation of silver nanoparticles was concurrently confirmed by taking the absorption spectra using a UV-visible spectrophotometer and the results are shown in Fig. 2a. Initially, the changes in  $\text{AgNO}_3$  solution colour from pale yellow to dark brown occurred within 2 h and signified the formation

of silver nanoparticles. In the presence of *Cyprus rotundas* root extract, the colour changes were observed due to excitation of surface plasmon resonance (SPR) at the surfaces of the silver nanoparticles. The typical SPR peak for silver nanoparticles was seen at 430 nm. The broad SPR peak observed at 430 nm represented the polydispersity of the materials. The experimental average particle size of the silver nanoparticles was monitored at  $58 \pm 0.05$  nm by the DLS measurements (Fig. 2b). The polydispersity index (PDI) of the measured solution was close to  $0.462 \pm 0.08$ .

The recorded FTIR spectra of *Cyprus rotundas* root extract and the silver nanoparticles are shown in Fig. 3a. FTIR measurements were carried out to identify the possible biomolecules present in the root broth that are usually responsible for capping and efficient stabilization of the solutions. The observed bands at 3420, 2934, 1715, 1643, 1400, 1074  $\text{cm}^{-1}$ , *etc.* clearly indicated the presence of alcohols, alkanes, aldehydes and ether groups or epoxy groups, respectively, in the solution,<sup>37</sup> which can help the nucleation process to reduce  $\text{Ag}^+$  to  $\text{Ag}^0$ . The peaks observed at 3420  $\text{cm}^{-1}$  and 1724  $\text{cm}^{-1}$  in the root extract were characteristic of O–H and C=O stretching vibrations, respectively. Besides, the absorption bands appearing at 1074  $\text{cm}^{-1}$  and 1400  $\text{cm}^{-1}$  represent the C–O stretching vibration present in alcohol, phenol, ether, ester and carboxylic acid groups. The appearance of weak bands at 2934  $\text{cm}^{-1}$  and 2854  $\text{cm}^{-1}$  in the spectrum of the extract indicated the presence of C–H stretching vibrations of the aliphatic  $-\text{CH}_2$  moiety. The appearance of a prominent high intensity

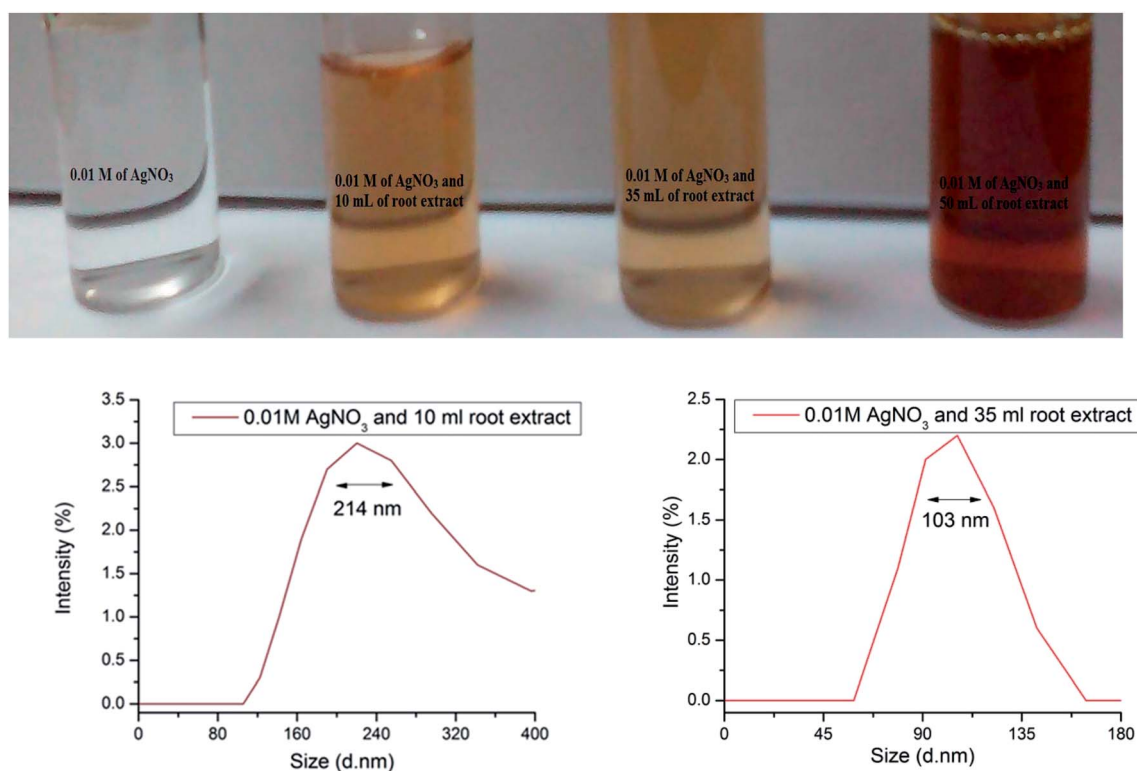


Fig. 1 Pictorial images and average particle-size distributions using DLS analysis of silver nanoparticles with variation of the amount of *Cyprus rotundas* root extract.



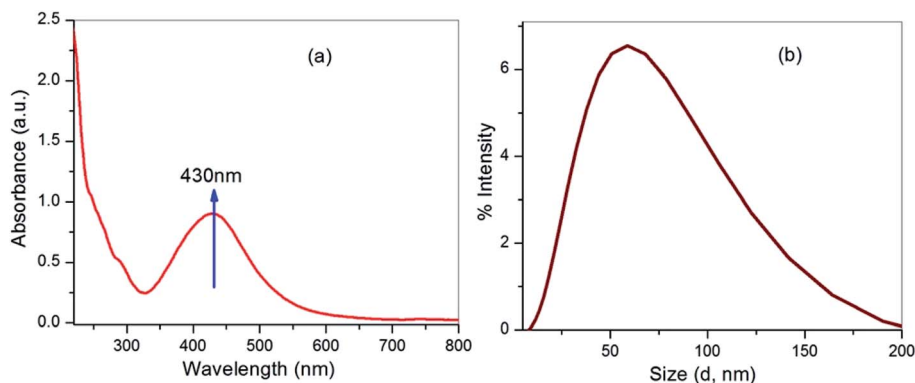


Fig. 2 (a) UV-vis spectrum and (b) average particle-size analysis of the silver nanoparticles.

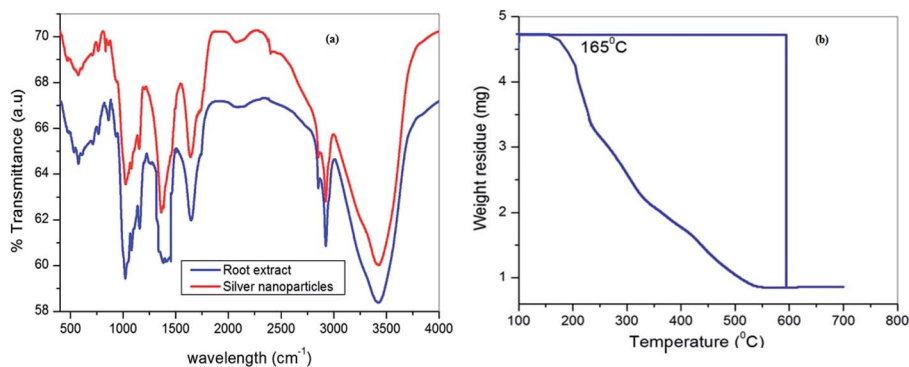


Fig. 3 (a) FTIR spectra of *Cyprus rotundas* root extract (blue line) and silver nanoparticles (red line); (b) thermogravimetric analysis of the silver nanoparticles.

peak and decrease in their intensity after the formation of nanoparticles manifested the aptitude of the strong binding interactions of the capping agent without any agglomeration. The thermogravimetric analysis (TGA) results in Fig. 3b were recorded on a Shimadzu TG 50 analyzer under a constant nitrogen flow ( $30 \text{ mL min}^{-1}$ ) at a heating rate of  $10 \text{ }^\circ\text{C min}^{-1}$ . Fig. 2b represents the weight loss of the solution in the 165–550  $^\circ\text{C}$  temperature range and the amount of weight loss was found to be 21.16%. This may be due to the desorption of the bio-organic compounds of the root extract. However, the present synthesized nanoparticles represented a stable form up to a very high temperature range.

In general, nanoparticles have shown unique properties related to their particle size. Transmission electron microscopy (TEM) is an excellent technique to analyze the accurate particle size of the prepared nanoparticles. Therefore, the size and morphology of the silver nanoparticles were further monitored using HRTEM analysis and the results are shown in Fig. 4a. Here, most of the silver nanoparticles were found to be spherical in shape and were uniformly dispersed without any agglomeration. The diameters of the silver nanoparticles ranged between 5–20 nm. The monitored nanoparticles size from using DLS and HRTEM analysis was found to be mismatched. The HR-TEM analysis images showed a very tiny portion of the sample with the possibility of the presence of

a few particles being present in the nanoparticles solution. However, DLS measures the relaxation time for the decay of the autocorrelation function of the scattered light, from which the diffusion coefficient is inversely proportional to the average particle size of the materials. In Fig. 4b, the selected area electron diffraction (SAED) patterns demonstrated the presence of bright spots within the concentric diffraction rings corresponding to the (200) plane of the face-centred-cubic (fcc) lattice of silver nanoparticles. The crystalline nature of the single silver nanoparticles is further shown in Fig. 4c and d, while the inverse fast Fourier transform (IFFT) images ascertained the layer spacing of silver nanoparticles was close to 0.21 nm.

### 3.3 Larvicidal activity

Nowadays, controlling mosquito disease vectors is an important aspect for the comfort of human health. In concern to environment issues, conventional synthetic insecticides present serious threats all over the world. In general, the use of herbal plants is one of the best alternatives to control mosquito vectors.<sup>38,39</sup> However, the bioactive compounds present in phytochemical extracts are not resistant to their medicinal properties due to presence of toxicity and biodegradability issues at higher dose concentrations.<sup>40</sup> Therefore, with the evolution of material science, the uses of metal nanoparticles are being developed to overcome these hazardous



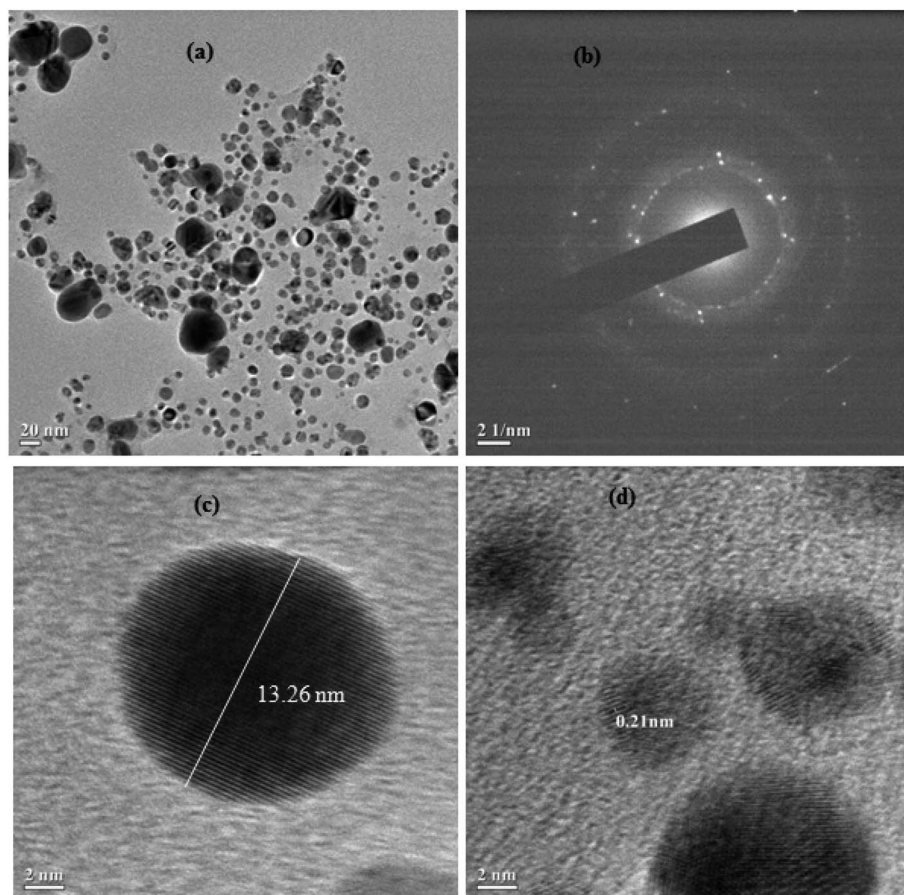


Fig. 4 (a) HRTEM images of *Cyprus rotundas* root extract-stabilized silver nanoparticles; (b) SAED images of randomly selected silver nanoparticles; (c) HRTEM images of single silver nanoparticles; (d) IFFT images of silver nanoparticles, also showing the layer spacing.

environmental issues. However, there are several factors that can affect their effectiveness; for example, the dose concentration range, particle-size distribution, bioavailability and stability as well as solvent medium used to prepare the nanoparticles.<sup>41</sup> In view of these factors, we chose a medicinal and rich bioresource-based material, *i.e.* *Cyprus rotundas* root, and prepared an aqueous root extract by using a facile hydrolysis method to synthesize the silver nanoparticles.

Initially, we monitored the efficacy of the materials against *Aedes albopictus* mosquito larvae with varying amounts of root extract, as shown in Fig. 1. It was observed that the amount of nanoparticles required for the mortality was 100 times higher than that of the optimized form. The optical images of both the treated and untreated larvae are shown in Fig. 5. In the case of the treated larvae 2, we can see that the nanoparticles had deeply penetrated into the larvae body due to the smaller size of the nanoparticles, whereas such a kind of observation was found to be missing for the untreated larvae and the treated larvae 1. Therefore, we further carried out our studies using the nanoparticles prepared through the 50 mL of root extract. We observed an excellent effect in terms of the bioefficacy of these materials against different mosquito disease vectors at very low dose concentrations and the obtained results are discussed in the following sections. The larvicidal activities of the nanoparticles were tested against the 3<sup>rd</sup> and 4<sup>th</sup> instars larvae of the

*Aedes albopictus*, *Aedes aegypti*, *Culex quinquefasciatus* and *Anopheles stephensi* mosquito vectors. The observed rates of mortality are further listed in Table 1. It could be seen that the maximum percentage of mortality occurred for all those species at 0.68 mg L<sup>-1</sup> solution of the synthesized silver nanoparticles.

The average rates of mortality for all three replicates were further subjected to probit regression analysis and the lethal concentrations calculated (LC<sub>50</sub> and LC<sub>90</sub>) in mg L<sup>-1</sup>. The results are shown in Table 2, where it can be seen that the lethal dose concentrations at the lower confidence limit (LC<sub>50</sub>) and at the upper confidence limit (LC<sub>90</sub>) with 95% fiducial limits of silver nanoparticles lay within the ranges of 0.05–0.225 mg L<sup>-1</sup> and 0.675–2.75 mg L<sup>-1</sup>, respectively. Compared with the reported literature data, the present synthesized silver nanoparticles had a higher rate of bioefficacy against mosquito larvae at very low dose concentrations. For example, Veerakumar *et al.* used *Sida acuta* leaves to synthesize silver nanoparticles and reported their larvicidal activity against *A. stephensi*, *A. aegypti*, and *C. quinquefasciatus* mosquito vectors.<sup>42</sup> The reported dose concentrations followed LC<sub>50</sub> and LC<sub>90</sub> values at 21.92 and 41.07 mg L<sup>-1</sup>; 23.96 and 44.05 mg L<sup>-1</sup>; 26.13 and 47.52 mg L<sup>-1</sup>, respectively. Raman *et al.* reported the effectiveness of silver nanoparticles using *Pithecellobium dulce* extract against the *C. quinquefasciatus* mosquito vector, which was mainly due to their higher surface-to-volume ratio, with an



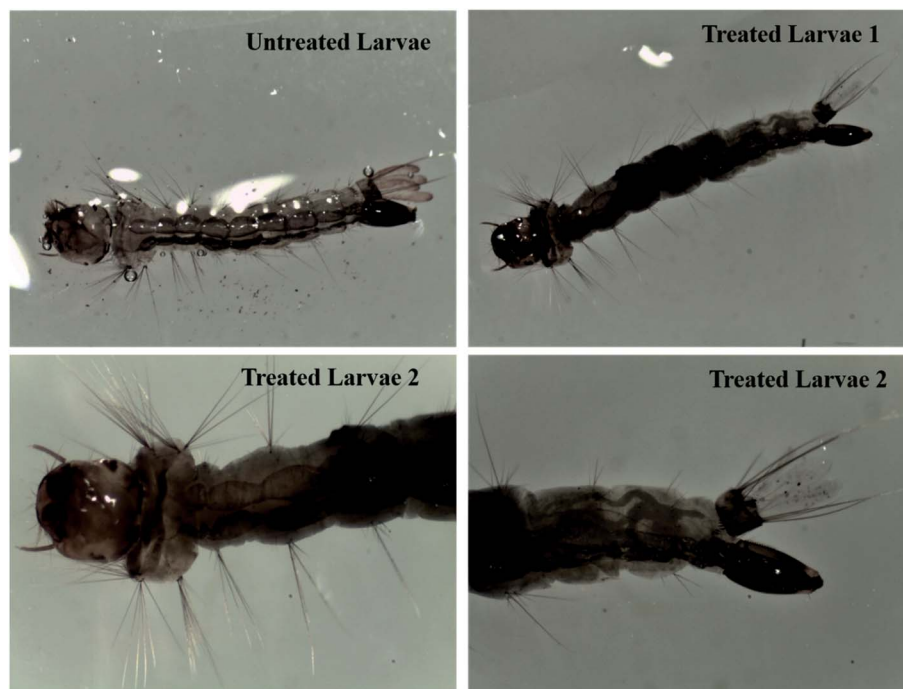


Fig. 5 Optical images of the untreated and treated *Aedes albopictus* mosquito larvae using varying amounts of root extract, i.e., 35 mL of root extract (treated larvae 1) and 50 mL of root extract (treated larvae 2) applied for the preparation of the nanoparticles.

Table 1 Larvicidal activity of the silver nanoparticles against both third and fourth instars larvae of *Aedes albopictus*, *Aedes aegypti*, *Culex quinquefasciatus* and *Anopheles stephensi* (control: nil mortality)

Dose (mg L <sup>-1</sup> )	Mosquito species							
	<i>A. albopictus</i>		<i>A. aegypti</i>		<i>C. quinquefasciatus</i>		<i>A. stephensi</i>	
	3 <sup>rd</sup> instars larvae	4 <sup>th</sup> instars larvae						
<b>% Mortality (mean value of three replicates, n = mean ± standard error)</b>								
1.0 mg L <sup>-1</sup>	100 ± 0.0	100 ± 0.0	100 ± 0.0	100 ± 0.0	100 ± 0.0	100 ± 0.0	100 ± 0.0	100 ± 0.0
0.50 mg L <sup>-1</sup>	81.3 ± 1.3	85.6 ± 4.3	80.9 ± 2.1	81.1 ± 2.9	82.9 ± 0.13	84.9 ± 4.6	80.4 ± 5.2	83.7 ± 5.2
0.30 mg L <sup>-1</sup>	69.1 ± 4.3	75.7 ± 2.9	72.5 ± 3.1	74.9 ± 1.3	71.9 ± 1.9	75.9 ± 2.9	71.8 ± 4.1	74.2 ± 1.1
0.10 mg L <sup>-1</sup>	51.9 ± 2.13	59.2 ± 2.8	55.1 ± 3.1	53.1 ± 4.0	58.0 ± 3.1	59.1 ± 4.1	52.6 ± 4.7	56.2 ± 4.2
0.05 mg L <sup>-1</sup>	31.7 ± 3.5	38.0 ± 2.9	36.1 ± 5.5	33.1 ± 1.5	37.1 ± 4.7	34.7 ± 5.1	34.1 ± 1.0	35.1 ± 2.9
0.03 mg L <sup>-1</sup>	15.1 ± 3.3	19.4 ± 5.1	16.9 ± 1.7	15.9 ± 1.0	17.9 ± 4.1	14.9 ± 0.9	19.8 ± 2.9	18.1 ± 4.5

LC<sub>50</sub> value of 21.56 mg L<sup>-1</sup>.<sup>43</sup> Rawani *et al.* reported that silver nanoparticles synthesized from aqueous extracts of dry leaves, fresh leaves and berries of *Solanum nigrum* showed LC<sub>50</sub> values of 1.33, 1.59 and 1.56 mg L<sup>-1</sup> respectively against *A. stephensi* vectors.<sup>44</sup> Whereas the LC<sub>90</sub> values were reported to be 3.97, 7.31 and 4.76 mg L<sup>-1</sup> against the *A. stephensi* vectors, respectively. They suggested that due to the smaller size of silver nanoparticles, they could easily pass through the epithelial membrane of mosquito vectors and inactivate the enzymatic pathway, then leading to cell death. Kumar *et al.* studied the larvicidal activity of synthesized silver nanoparticles using *Morinda tinctoria* extract against *C. quinquefasciatus* species, where their reported LC<sub>50</sub> value was 1.44 mg L<sup>-1</sup>.<sup>45</sup> Furthermore, synthesized silver nanoparticles using a herbicidal plant

extracts, like *Tinospora cordifolia* (LC<sub>50</sub> ~ 6.35 mg L<sup>-1</sup>) and *Nelumbo nucifera* (LC<sub>50</sub> ~ 0.69 mg L<sup>-1</sup>), showed potential larvicidal activity against *A. stephensi* and *C. quinquefasciatus* larvae, respectively.<sup>46,47</sup> Similarly, the reported silver nanoparticles synthesized from the bark of *A. indica* (Neem) were also tested for larvicidal and pupicidal activities against the malaria vector *A. stephensi* and filariasis vector *C. quinquefasciatus*,<sup>48</sup> where the 1<sup>st</sup> and 2<sup>nd</sup> instars larvae of *C. quinquefasciatus* had 100% mortality after 30 min exposure to the nanoparticles. However, pupicidal activity was observed at an LC<sub>50</sub> of 4 mg L<sup>-1</sup> for *A. stephensi* and *C. quinquefasciatus* vectors, whereas their LC<sub>90</sub> values were recorded at 11 and 13 mg L<sup>-1</sup>, respectively, after 3 h exposure. Vimala *et al.* synthesized silver nanoparticles using *Couroupita guianensis* leaf extract and reported their



**Table 2** Lethal concentrations (LC<sub>50</sub> (mg L<sup>-1</sup>) (LCL–UCL) and LC<sub>90</sub> (mg L<sup>-1</sup>) (LCL–UCL)) of the silver nanoparticles against both third and fourth instars larvae of *Aedes albopictus*, *Aedes aegypti*, *Culex quinquefasciatus* and *Anopheles stephensi*

Dose (mg L <sup>-1</sup> )	Mosquito species							
	<i>A. albopictus</i>		<i>A. aegypti</i>		<i>C. quinquefasciatus</i>		<i>A. stephensi</i>	
	3 <sup>rd</sup> instars larvae	4 <sup>th</sup> instars larvae	3 <sup>rd</sup> instars larvae	4 <sup>th</sup> instars larvae	3 <sup>rd</sup> instars larvae	4 <sup>th</sup> instars larvae	3 <sup>rd</sup> instars larvae	4 <sup>th</sup> instars larvae
LC <sub>50</sub> (mg L <sup>-1</sup> )	0.078	0.077	0.139	0.210	0.133	0.126	0.223	0.218
(LCL–UCL) <sup>a</sup>	(0.05–0.12)	(0.05–0.11)	(0.09–0.20)	(0.14–0.34)	(0.09–0.18)	(0.09–0.18)	(0.16–0.34)	(0.15–0.31)
LC <sub>90</sub> (mg L <sup>-1</sup> )	0.674	0.686	1.028	2.730	0.930	0.904	1.507	1.34
(LCL–UCL) <sup>a</sup>	(0.40–1.50)	(0.41–1.55)	(0.62–2.29)	(0.29–10.37)	(0.57–2.05)	(0.55–1.95)	(0.62–2.29)	(0.79–1.57)

<sup>a</sup> Lethal concentration for silver nanoparticle-treated larvae, LCL – lower concentration limit, UCL – upper concentration limit.

extensive mortality rate, with LC<sub>50</sub> at 2.1 mg L<sup>-1</sup> and LC<sub>90</sub> at 5.59 mg L<sup>-1</sup>.<sup>49</sup>

Amongst all those recent studies of silver nanoparticles, here we report the exclusive effectiveness of our present silver nanoparticles materials, where LC<sub>50</sub> and LC<sub>90</sub> values were recorded at very low concentrations, *i.e.* 0.05 mg L<sup>-1</sup> and 0.68 mg L<sup>-1</sup>, respectively. These may be due to the presence of stable and highly photoinduced-based synthesized nanoparticles materials that could be uniformly distributed into the larval body because of their smaller sizes. Despite the number of literature reports about the larvicidal activity of silver nanoparticles, it is very rare to find details of the life history traits of these materials owing to issues around the toxicity and poor stability of the reported nanoparticles till date. Therefore, we extended our studies to examine the life history traits assay of mosquito vectors followed by their an investigation into their mechanism.

### 3.4 Life history trait assays of nanoparticles-treated mosquito species

A series of experiments was carried out in the present investigation to quantify the complete life cycle traits by assay of

mosquito species, including their survival rate and fitness consequences after treatment. The overall experiments were carried out at 28 ± 2 °C and 75–85% relative humidity under 14 : 10 light and dark photoperiods at variable concentrations of the nanoparticles. Since the nanoparticles-treated larvae near the concentration range of the LC<sub>50</sub>, *i.e.* at 0.05–0.225 mg L<sup>-1</sup>, showed 100% mortality within 48–72 h, we chose the concentration range of nanoparticles near the LC<sub>30</sub>, *i.e.* 0.02 mg L<sup>-1</sup>, to understand the life history traits by assay of *A. albopictus* and *C. quinquefasciatus* larvae. Initially, the survival rate for the treated larvae were recorded within a fixed period of time and compared with untreated larvae under identical conditions. Interestingly, only 30% of the treated larvae survived to complete their life cycle under the same circumstances (Fig. 6A). However, 70% of them had a delayed life cycle growth and stayed in the larvae stage up to a minimum of 30 days and then they showed fatality at that stage. While the untreated larvae species completed their whole life cycle stages within a very short period of time (1–12 days). A comparative survival rate study of nanoparticles-treated and untreated larvae is shown in Fig. 6B. Fig. 4b shows the significant linear fitting data of the nanoparticles-treated larvae, where the calculated

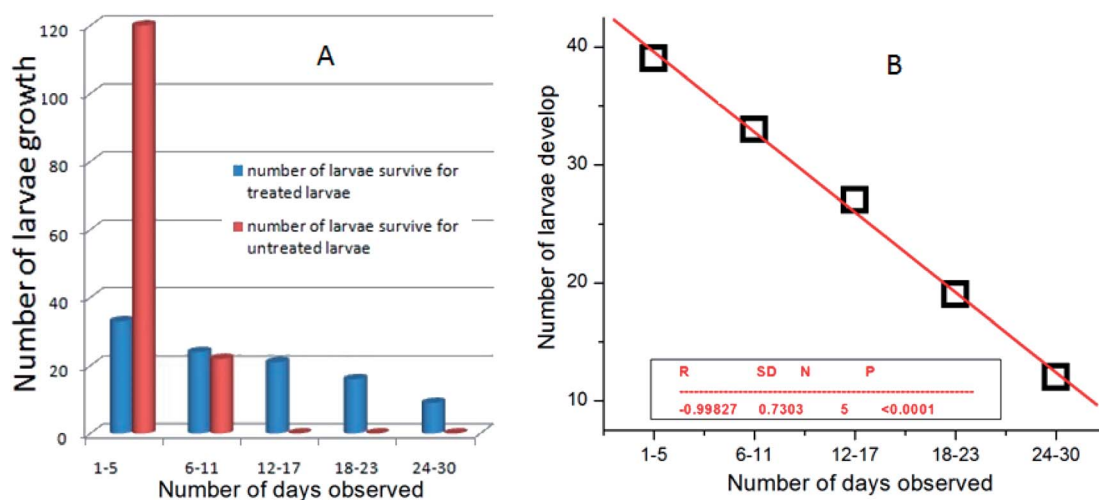


**Fig. 6** (A) Plots of the number of *Culex quinquefasciatus* larvae developed for both the treated and untreated larvae and (B) linear fitted data of the silver nanoparticle-treated larvae.



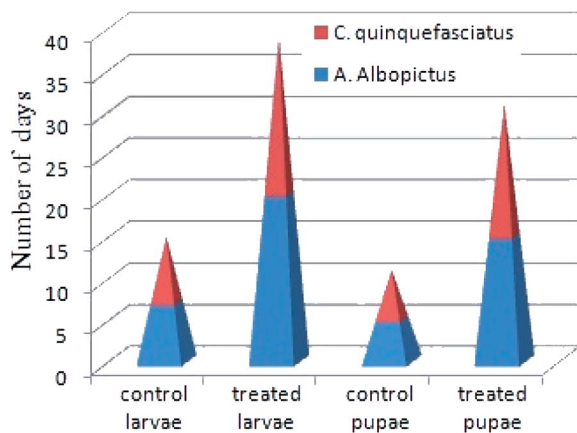


Fig. 7 Survival rates of *A. albopictus* and *C. quinquefasciatus* mosquito species of the control and silver nanoparticle-treated larvae and pupae at the range of the  $LC_{30}$  dose concentration.

probability of the findings ( $P$ ) and regression time ( $R$ ) were found to be  $<0.0001$  and  $-0.0998$ , respectively. The reported  $P$  and  $R$  values in Fig. 6B indicate the accuracy of the present experimental results.

In addition, to understand the physical fitness level of those 30% surviving mosquito larvae in both the treated and untreated stage, we collected them and further transferred them into two different cages and allowed them to emerge as adults. The number of days required to complete their life cycle stages was recorded.

In Fig. 7, it is shown that in comparison to untreated larvae, the treated larvae took a longer period of time to complete their life cycles. For instance, the 3<sup>rd</sup> instars of untreated larvae generally took up to 7–12 days to become pupae, whereas the treated larvae took up to 18–40 days. Similarly, the treated larvae at the pupae stage took 15–28 days to become adults. In this case, we can say that after the treatment of  $0.02 \text{ mg L}^{-1}$  concentration of nanoparticles materials, those 30% surviving larvae also had an impaired growth capability to complete their life cycles. In contrast to the studies performed by Koella *et al.*, we can expect that the present nanoparticles materials incurred an immunological stress in the earlier stages of the treated larvae at that particular dose concentration, which then caused

a delay in their life cycle stages.<sup>50</sup> In addition, the possibility of bond formation between the nanoparticles materials and the sulphur- or phosphorous-containing compounds, like DNA, proteins, *etc.*, present in the mosquito species can also inhibit their enzymatic actions, leading to cell death after a short interval of time.<sup>51</sup>

### 3.5 Fecundity and hatchability rate studies of the silver nanoparticles-treated larvae

In continuing the life history traits analysis, the fecundity and hatchability rate of the nanoparticles-treated pupae were also kept under observation and compared with the same rate for the untreated mosquito species. Upon emergence as adults, both the surviving treated and untreated pupae of the above experiments were separated out in two different cages and provided 10% honey solutions for sustenance and a blood meal prior to the female mosquito adult producing eggs. Under one week observation, the produced eggs were further collected and kept in two different enamel trays for hatching new larvae from the treated and untreated species. It was interesting to note that, those eggs collected from the nanoparticles-treated *A. albopictus* and *C. quinquefasciatus* adult mosquitoes did not hatch to start their new life cycle. However, the control mosquitoes eventually hatched and started their life cycle within a very short period of time. Therefore, this could further suggest that due to the probable disturbance of their enzymatic pathways, those surviving mosquitoes after treatment with the nanoparticles did not even start their new life cycle. Furthermore, the studies were extended to manifest the reduced formation of egg masses and diminished hatching of eggs by varying the dose concentration below the  $LC_{30}$ . Therefore, we observed these activities at different concentrations ranging from  $0.001$ – $0.01 \text{ mg L}^{-1}$  and the results are shown in Table 3. At  $0.01 \text{ mg L}^{-1}$  concentration of nanoparticles, the numbers of egg masses were reduced to  $2.03 \pm 0.07$  and  $1.76 \pm 0.15$  for *A. albopictus* and *C. quinquefasciatus* respectively as compared to  $10.00 \pm 0.00$  egg masses in the case of the control. Whereas, at  $0.005$  and  $0.001 \text{ mg L}^{-1}$  concentrations, the egg masses laid were  $8.23 \pm 0.09$  and  $5.19 \pm 0.21$  for *A. albopictus*; while similar reduced values of  $8.36 \pm 0.17$  and  $4.96 \pm 0.12$  were found for the *C. quinquefasciatus*

Table 3 Effect of the silver nanoparticles against the fecundity and egg hatching rate of *A. albopictus* and *C. quinquefasciatus* mosquito species

Dose ( $\text{mg L}^{-1}$ )	Species	Number of egg masses laid	Number of eggs	Total number of egg laid	Number of eggs hatched	Percentage hatching of eggs
		Mean $\pm$ SE	Mean $\pm$ SE	Mean $\pm$ SE	Mean $\pm$ SE	Mean $\pm$ SE
0.001 $\text{mg L}^{-1}$	<i>A. albopictus</i>	$8.23 \pm 0.09$	$317.0 \pm 0.98$	$2162.53 \pm 3.12$	$216.60 \pm 0.57$	$64.23 \pm 0.92$
	<i>C. quinquefasciatus</i>	$8.36 \pm 0.17$	$319.0 \pm 0.76$	$2675.13 \pm 2.90$	$199.44 \pm 0.39$	$69.68 \pm 0.41$
0.005 $\text{mg L}^{-1}$	<i>A. albopictus</i>	$5.19 \pm 0.21$	$257.0 \pm 0.21$	$1622.44 \pm 5.22$	$126.22 \pm 0.71$	$48.03 \pm 0.08$
	<i>C. quinquefasciatus</i>	$4.96 \pm 0.12$	$243.0 \pm 0.34$	$1475.61 \pm 4.30$	$115.56 \pm 0.88$	$42.89 \pm 0.68$
0.010 $\text{mg L}^{-1}$	<i>A. albopictus</i>	$2.03 \pm 0.07$	$97.0 \pm 0.14$	$672.52 \pm 1.16$	$39.27 \pm 0.11$	$17.23 \pm 0.71$
	<i>C. quinquefasciatus</i>	$1.76 \pm 0.15$	$89.0 \pm 0.20$	$499.81 \pm 1.35$	$35.10 \pm 0.44$	$19.55 \pm 0.99$
Control	<i>A. albopictus</i>	$10.0 \pm 0.00$	$417.0 \pm 0.58$	$3647.22 \pm 3.12$	$365.66 \pm 0.53$	$89.99 \pm 1.23$
	<i>C. quinquefasciatus</i>	$10.0 \pm 0.00$	$423.0 \pm 0.36$	$3915.13 \pm 3.68$	$398.22 \pm 0.41$	$89.83 \pm 1.09$



mosquito species. The significant reduction of eggs in each egg mass was monitored at all the concentrations of silver nanoparticles. The numbers of eggs laid per egg mass were  $97.0 \pm 0.14$  and  $89.0 \pm 0.20$  for *A. albopictus* and *C. quinquefasciatus* mosquitoes as compared to  $417.0 \pm 0.58$  and  $423.0 \pm 0.36$  for the control, respectively. Similarly, at 0.001 and 0.005 mg L<sup>-1</sup> concentrations, the eggs laid per egg mass were  $317.0 \pm 0.98$  and  $257.0 \pm 0.21$  for *A. albopictus*, whereas the same values were  $319.0 \pm 0.76$  and  $243.0 \pm 0.34$  for *C. quinquefasciatus*, respectively. The total number of eggs laid by female mosquitoes also diminished when a nanoparticles-treated diet was provided to them. In the case of the untreated experiment,  $3647.22 \pm 3.12$  and  $3915.13 \pm 3.68$  eggs for *A. albopictus* and *C. quinquefasciatus* were laid, which were decreased by up to  $672.52 \pm 1.16$  and  $499.81 \pm 1.35$  at 0.01 mg L<sup>-1</sup> of nanoparticles mixtures, respectively. Likewise, at 0.001 and 0.005 mg L<sup>-1</sup> of nanoparticles mixtures, the eggs laid were reduced to  $2162.53 \pm 3.12$  and  $2675.13 \pm 2.90$  for *A. albopictus*;  $2675.13 \pm 2.90$  and  $1475.61 \pm 4.30$  for *C. quinquefasciatus*, respectively. The percentage hatching of the eggs was also affected by feeding on a nanoparticles-treated diet, whereby the maximum egg hatching was approximately 19% at 0.01 mg L<sup>-1</sup> of nanoparticles mixture, which further increased with the decrease in concentration of the solution. Therefore, the overall studies demonstrated that when adult females of *A. albopictus* and *C. quinquefasciatus* mosquitoes were fed silver nanoparticles-treated diets, a drastic change in fecundity and the egg hatching rate occurred. Thus the tremendous anti-ovicidal effectiveness of the synthesized silver nanoparticles materials against various mosquito species may be increased due to the presence of *Cyprus rotundas* root extract, which contains various carbohydrate contents, like  $\alpha$ -cyperone,

$\beta$ -selinene, cyperene, patchoulenone, sugeonol, kobusone and isokobusone *etc.*, to enhance their properties.

The deterrent activity was directly proportional to the concentration of the nanoparticles mixtures. The present investigations are compatible with the previously reported studies of plant or oil extract materials and their derivatives. For example, Pushpalatha *et al.* reported that the fecundity rates of *C. quinquefasciatus* were decreased by up to 72.4% and 85.4% over the control at 50 ppm concentrations of *Croton hirtus* and *Pogostemon quadrifolius* leaf extract, respectively.<sup>52</sup> Similarly, inflorescence oil extract of *Piper marginatum* did not show anti-oviposition effectiveness towards *A. aegypti* females at 50 ppm.<sup>53</sup> In contrast to these reported data, the present results of our work indicate an onsite potency of the nanoparticles mixture at very low dose concentrations, *i.e.* 0.001 mg L<sup>-1</sup> (0.001 ppm). Therefore, one can speculate that the use of such a sustainable nanoweapon to control the aforesaid vectors has immense potential against mosquito vectors in the practical field of applications. However, further studies on the mechanistic actions of the nanoparticles mixtures are also required for the development of such onsite biolarvicidal agents.

### 3.6 Histological studies of nanoparticles-treated and untreated larvae

To understand the morphological activity of the nanoparticles-treated mosquito vectors, we further investigated the histological studies of *Aedes albopictus* larvae. In Fig. 8A–C, it can be seen that for the untreated larvae, the dark intercellular structure of the *Aedes albopictus* larvae along with their plasma membrane and nuclei are in the normal form; whereas for the nanoparticles-treated larvae, dramatic changes have occurred towards the intercellular larval body structures, which indicates that due to the

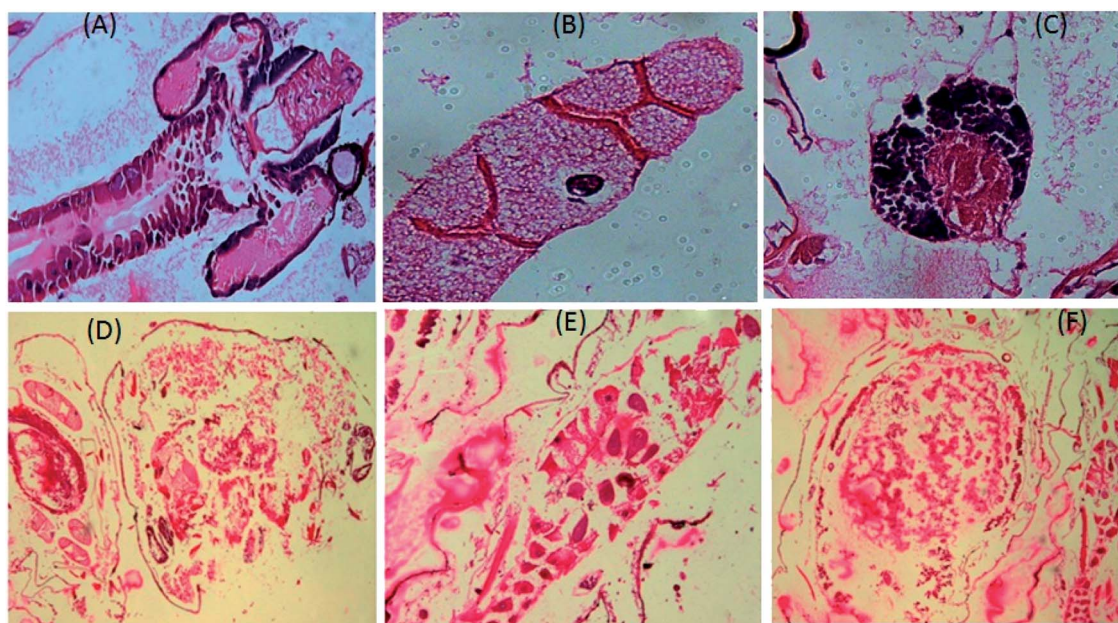


Fig. 8 Longitudinal section of both untreated (A–C) and silver nanoparticle-treated (D–F) third instars larvae of *Aedes albopictus*.



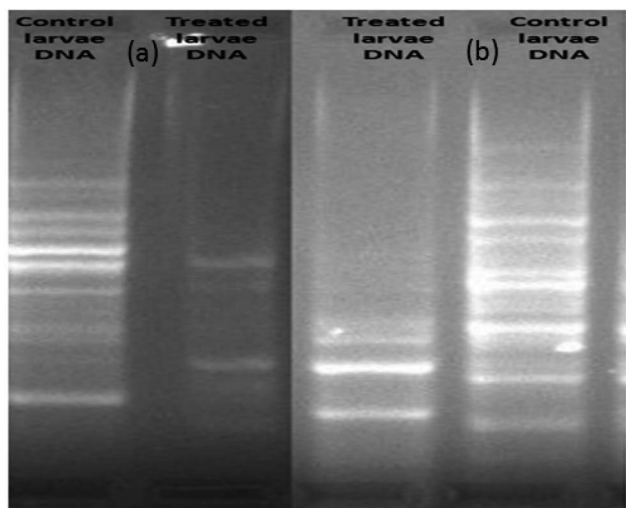


Fig. 9 Comparison of the RAPD-PCR profiles of 3<sup>rd</sup> instars larvae of untreated and silver nanoparticle-treated *A. albopictus* larvae. (a) Primer 1: (GTGGCTTGGA) and (b) primer 2 (GTAAACCGCC).

penetration of silver nanoparticles into the larval body, the internal body textures have been gradually damaged. Also with the increase in time, the nanoparticles mixtures spread further into the overall body part of the larvae and by then with mixing the gut contents with the haemolymph of the larvae body eventually cause cell death.<sup>11,54</sup> In addition, there is also a possibility of disturbing the enzymatic pathways for destruction of the larvae cells.<sup>54</sup>

### 3.7 RAPD assay for the detection of DNA damage of the treated larvae

The extracted DNA samples of 3<sup>rd</sup> instars *A. albopictus* larvae were exposed to silver nanoparticles at the LC<sub>50</sub> dose and their DNA band was evaluated. Initially, 20 numbers of RAPD primers were screened with a laboratory-reared strain of *A. albopictus* mosquito larvae in order to find a suitable primer that could be used further to generate the fingerprints of *A. albopictus* mosquito species. Out of these, only two primers, assigned here as primer 1 and primer 2, generated clear and discrete banding patterns with the laboratory-reared *A. albopictus* mosquito DNA. Both the primers had reproducible results with their genetic fingerprints obtained with the agarose gel. It was interesting to note that the observed numbers of bands for the nanoparticles-treated larvae dramatically decreased with the breakage of their strands as compared to the control larvae (Fig. 9).

Therefore, the genomic alteration analysis of the silver nanoparticles-treated larvae revealed the modifications of the RAPD patterns and the changes of the primer binding sites of the *A. albopictus* mosquito. As a result, structural changes took place due to the DNA damage of *A. albopictus* larvae. Besides, the changes observed in the RAPD profile treatment, including the loss of various bands, also indicated the formation of covalent bonds between the nanoparticles mixtures and the S- or N-atoms present in the DNA of the larvae.<sup>55</sup> In consequence, this leads to mutational or cytogenetic changes inside the larval body, which can lead to cell death.

## 4. Conclusions

The present work demonstrated the efficacy of a sustainable bioresource-based nanoparticles material to control the larvicidal activity of mosquito vectors. The larvicidal activity of silver nanoparticles against various common mosquito species, like *Aedes albopictus*, *Anopheles stephensi* and *Culex quinquefasciatus*, was observed at very low concentrations of nanoparticles. A facile and ecofriendly method was established to synthesize the materials using aqueous *Cyprus rotundas* root extract. The synthesized materials were demonstrated to be an efficient onsite biolarvicidal agent at very low dose concentrations, *i.e.* 0.001–0.02 mg L<sup>-1</sup>. *Cyprus rotundas* root contains several organic moieties, such as steroids, alkaloids, flavonoids, triterpenoids (terpenoids), saponin, coumarin and quinine, or other compounds, like myrcene, limonene, xanthatin, xanthinin, that help to generate surface-functionalized circumstances during preparation of the root extract and can lead to the formation of stable and highly photoinduced silver nanoparticles materials. The details of the life history traits by assay of the nanoparticles materials indicated the potential use of such a sustainable nanoweapon against the aforementioned mosquito vectors for practical field applications. The mechanistic actions of the nanoparticles were confirmed by histopathological and RAPD analyses. It could be seen that the nanomaterials could penetrate and be uniformly distributed in the larvae body. Thereby, it can affect their intracellular body functions and cause a respective effect of synergism. As a result, the present studies demonstrate the use of sustainable bioresource-based materials to promote a promising biolarvicidal candidate in the direction of controlling the serious threat of mosquito vectors around the world.

## Funding

This study was supported by the grant BT/518/NE/TBP/2013 dated Dec 12, 2014 (received from DBT, Govt. of India), DRL, Tezpur and DRDO, New Delhi. The funders had no role in study design, data collection and analysis, decision to publish, or preparation of the manuscript.

## Authors' contributions

PKR, DG and NS designed the study. NS performed the synthesis and characterization of materials. DG and BD performed mosquito larvicidal experiment. DD and SI performed histological studies. HKG and PSR were responsible for financial support. VT and PC reviewed the manuscript. All authors read and approved the final manuscript.

## Abbreviations

UV	Ultraviolet spectroscopy
FTIR	Fourier transforms infrared spectroscopy
DLS	Dynamic light scattering
TGA	Thermo gravimetric analysis



HRTEM	High-resolution transmission electron microscopy
RAPD	Random amplified polymorphic DNA
PCR	Polymerase chain reaction
DNA	Deoxyribonucleic acid

## Conflicts of interest

The authors declare that they have no competing interests.

## Acknowledgements

Authors are grateful to DBT, India for financial assistance through the grant BT/518/NE/TBP/2013 dated Dec 12, 2014. DRL, Tezpur and DRDO, New Delhi, are duly acknowledged for providing research platform and necessary permission. Authors are also grateful to Mr M. G. Vairale, Scientist-D, Botanist, DRL Tezpur for identify the grass used here.

## References

- P. K. Mittal and S. K. Subbarao, *ICMR Bull.*, 2003, **33**(4), 1–10.
- Filariasis, in *Ciba Foundation Symposium*, ed. J. W. Mak, D. Evered and S. Clark, John Wiley & Sons, Chichester, UK, 2007, vol. 127.
- N. Nitatpattana, C. Apiwathnasorn, P. Barbazan, S. Leemingsawat, S. Yoksan and J. Gonzalez, *Southeast Asian J. Trop. Med. Public Health*, 2005, **36**(4), 875–878.
- T. Mathivanan, K. Govindarajan, K. Elumalai and A. Ananthan, *J. Vector Borne Dis.*, 2000, **47**(3), 178–180.
- M. Tiwary, S. N. Naik, D. K. Tewary, P. K. Mittal and S. Yadav, *J. Vector Borne Dis.*, 2007, **44**(3), 198–204.
- J. M. Cohen, D. L. Smith, C. Cotter, A. Ward and G. Yamey, *Malar. J.*, 2012, **11**(2), 122–138.
- A. F. Howard, G. Zhou G and F. X. Omlin, *BMC Public Health*, 2007, **7**(1), 199–205.
- R. M. Al-Mehmadi and A. A. Al-Khalaf, *J. King Saud Univ.*, 2010, **22**(8), 77–85.
- C. Kamaraj, A. Abdul Rahman, A. Bagavan, A. Abduz Zahir, G. Elango, P. Kandan, G. Rajakumar, S. Marimuthu and T. Santhoshkumar, *Trop. Biomed.*, 2010, **27**(2), 211–219.
- N. Sultana, P. K. Raul, D. Goswami, B. Das, H. K. Gogoi and P. S. Raju, *Environ. Chem. Lett.*, 2018, **16**(3), 1017–1023.
- S. P. Chandran, M. Chaudhary, R. Pasricha, A. Ahmad and M. Sastry, *Biotechnol. Prog.*, 2006, **22**(2), 577–583.
- D. M. Ledwith, A. M. Whelan and J. M. Kelly, *J. Mater. Chem.*, 2007, **17**(2), 2459–2464.
- S. B. Brichkin, M. G. Spirin, L. M. Nikolenko, D. Y. Nikolenko and V. Y. Gak, *High Energy Chem.*, 2008, **42**(7), 516–521.
- F. Mafune, J. Kohno, Y. Takeda, T. Kondow and H. Sawabe, *J. Phys. Chem. B*, 2008, **104**(39), 8333–8337.
- S. Z. Malynych and G. Chumanov, *J. Vac. Sci. Technol., A*, 2003, **21**(3), 723–727.
- C. D. Patil, S. V. Patil, H. P. Borase, B. K. Salunke and R. B. Salunkhe, *Parasitol. Res.*, 2012, **110**(5), 1815–1822.
- K. Velayutham, A. A. Rahuman, G. Rajakumar, S. M. Roopan, G. Elango, C. Kamaraj, S. Marimuthu, T. Santhoshkumar, M. Iyappan and C. Siva, *Asian Pac. J. Trop. Med.*, 2013, **6**(2), 95–101.
- U. Muthukumar, M. Govindaraja and M. Rajeswary, *Parasitol. Res.*, 2015, **114**(5), 989–999.
- N. K. Mondal, A. Chowdhury, U. Dey, P. Mukhopadhyaya, S. K. Chatterjee Das and J. K. Datta, *Asian Pac. J. Trop. Dis.*, 2014, **4**(1), S204–S210.
- T. Elijah, O. Adesuji Omolara, O. Oluwaniyi Haleemat, I. Adegoke Roshila, M. Ayomide, H. Labulo Olusola, S. Bodede and O. Charles, *J. Nanomater.*, 2016, **2016**, 4363751.
- L. Sintubin, W. Verstraete and N. Boon, *Biotechnol. Bioeng.*, 2012, **109**(10), 2422–2436.
- S. Iravani, *Green Chem.*, 2011, **13**, 2638–2650.
- V. Kumar and S. K. Yadav, *J. Chem. Technol. Biotechnol.*, 2009, **84**(2), 151–157.
- S. Marimuthu, A. A. Rahuman, G. Rajakumar, T. Santhoshkumar and A. V. Kirthi, *Parasitol. Res.*, 2011, **108**(6), 1541–1549.
- K. Murugan, D. Jeyabalan, N. Senthilkumar, R. Babu and S. Sivaramkrishnan, *J. Entomol. Res.*, 1996, **20**, 137–139.
- E. K. Sohn, S. A. Johari, T. G. Kim, J. K. Kim, E. Kim, G. H. Lee, Y. S. Chung and J. Yu, *BioMed Res. Int.*, 2015, **20**(5), 1–12.
- N. Kumar, J. P. Singh, R. Ranjan, S. Devi and V. M. Srinivasan, *Adv. Appl. Sci. Res.*, 2013, **4**(4), 299–302.
- W. S. Abott, *J. Econ. Entomol.*, 1925, **18**, 265–266.
- D. J. Finney, *Probit analysis: a statistical treatment of the sigmoid response curve*, Cambridge University Press, University of Oxford, Cambridge, Oxford, England, 1947, pp. 256–258.
- L. Deng, S. Y. Koou, A. B. Png, L. C. Ng and S. G. Lam-Phua, *Trop. Biomed.*, 2012, **29**(1), 169–174.
- M. E. Ballinger-Crabtree, W. C. Black and B. R. Miller, *Am. J. Trop. Med. Hyg.*, 1992, **47**(6), 893–901.
- V. Tyagi, A. K. Sharma, R. Yadav, T. Adak, D. Sukumaran, O. P. Agrawal and V. Veer, *European Journal of Biotechnology and Bioscience*, 2015, **3**(8), 47–54.
- J. Sambrook, E. F. Fritsch and T. Maniatis, *Molecular Cloning. A Laboratory Manual*, Cold Spring Harbor Laboratory Press, Cold Spring Harbor NY, 2nd edn, 1989.
- M. Ishihara, V. Q. Nguyen, Y. Mori, S. Nakamura and H. Hattori, *Int. J. Mol. Sci.*, 2015, **16**(3), 13973–13988.
- N. Kumar, J. P. Singh, R. Ranjan, C. S. Devi and V. M. Srinivasan, *Adv. Appl. Sci. Res.*, 2013, **4**(4), 299–302.
- G. A. Mohamed, *Bull. Fac. Pharm.*, 2015, **53**(1), 5–9.
- B. Ajitha, A. R. Reddy and P. S. Reddy, *Mater. Sci. Eng., C*, 2015, **49**, 373–381.
- S. Tripathu, D. Pradhan and M. Anjan, *Int. J. Pharm. Biol. Sci.*, 2013, **1**(5), 1–7.
- M. Govindarajan, R. Sivaakumar, M. Rajeswary and K. Yogalakshmi, *Asian Pac. J. Trop. Dis.*, 2012, **2**(2), 124–128.
- M. E. Mohammed, *Journal of Entomology and Zoology Studies*, 2016, **4**(2), 483–488.
- S. Agnihotri and S. Mukherji, *Nanoscale*, 2013, **5**, 7328–7340.
- K. Veerakumar, M. Govindarajan and M. Rajeswary, *Parasitol. Res.*, 2013, **112**(12), 4073–4085.



- 43 N. Raman, S. Sudharsan, V. Veerakumar, N. Pravin and K. Vithiya, *Spectrochim. Acta, Part A*, 2012, **96**, 1031–1037.
- 44 A. Rawani, A. Ghosh and G. Chandra, *Acta Trop.*, 2013, **128**(3), 613–622.
- 45 R. K. Kumar, R. Nattuthurai, J. Gopinath and T. Mariappan, *Parasitol. Res.*, 2014, **14**(2), 411–417.
- 46 T. Santhoshkumar, A. A. Rahuman, G. Rajakumar, A. Marimuthu Bagavan, C. Jayaseelan, A. A. Zahir, G. Elango and C. Kamaraj, *Parasitol. Res.*, 2011, **108**(3), 693–702.
- 47 S. Mitra, S. Chandra, P. Patra, P. Pramanik and A. Goswami, *J. Mater. Chem.*, 2011, **21**, 17638–17641.
- 48 N. Soni and S. Prakash, *Parasitol. Res.*, 2014, **113**(11), 4015–4022.
- 49 R. T. V. Vimala, G. Sathishkumar and S. Sivaramakrishnan, *Spectrochim. Acta, Part A*, 2015, **135**, 110–115.
- 50 J. C. Koella and C. Boette, *Evolution*, 2002, **56**(5), 1074–1079.
- 51 R. Srinivasan, D. Nataranjan, S. Karthi and M. S. Shivakumar, *International Journal of Mosquito Research*, 2014, **1**(4), 66–71.
- 52 E. Pushpalatha, *Adv. Zool. Bot.*, 2015, **3**(3), 38–41.
- 53 E. S. Autran, I. A. Neves, C. S. D. Silva, G. K. Santos, C. S. D. Camara and D. M. Navarro, *Bioresour. Technol.*, 2003, **100**(1), 2284–2288.
- 54 G. Sutter and E. S. Raun, *J. Invertebr. Pathol.*, 1967, **9**, 90–103.
- 55 C. Jones and A. Kortenkamp, *Teratog., Carcinog., Mutagen.*, 2000, **20**(2), 49–63.

